

The $^{44}\text{Ti}(\alpha, p)$ Reaction and its Implication on the ^{44}Ti Yield in Supernovae

A. A. Sonzogni,¹ K. E. Rehm,¹ I. Ahmad,¹ F. Borasi,² D. L. Bowers,¹ F. Brumwell,¹ J. Caggiano,¹ C. N. Davids,¹ J. P. Greene,¹ B. Harss,¹ A. Heinz,¹ D. Henderson,¹ R. V. F. Janssens,¹ C. L. Jiang,¹ G. McMichael,¹ J. Nolen,¹ R. C. Pardo,¹ M. Paul,³ J. P. Schiffer,¹ R. E. Segel,² D. Seweryniak,¹ R. H. Siemssen,¹ J. W. Truran,⁴ J. Uusitalo,¹ I. Wiedenhöver,¹ and B. Zabransky¹

¹Argonne National Laboratory, 9700 South Cass Avenue, Argonne, Illinois 60439

²Northwestern University, Evanston, Illinois 60208

³Hebrew University, Jerusalem, Israel

⁴Department of Astronomy and Astrophysics, University of Chicago, 5640 South Ellis Avenue, Chicago, Illinois 60637

(Received 15 October 1999)

Cross sections for the $^{44}\text{Ti}(\alpha, p)^{47}\text{V}$ reaction which significantly affects the yield of ^{44}Ti in supernovae were measured in the energy range $5.7 \text{ MeV} \leq E_{\text{c.m.}} \leq 9 \text{ MeV}$, using a beam of radioactive ^{44}Ti . The cross sections and the deduced astrophysical reaction rates are larger than the results from theoretical calculations by about a factor of 2. The implications of this increase in the reaction rate for the search of supernovae using space-based gamma detectors are discussed.

PACS numbers: 26.30.+k, 25.60.Dz, 25.60.Je, 26.50.+x

The nucleus of ^{44}Ti is of great importance in nuclear astrophysics [1,2]. Nuclei of ^{44}Ti are produced in the last stages of a supernova event in the so-called alpha-rich freeze-out [1]. The recent observation of γ rays associated with the decay of ^{44}Ti by the COMPTEL space telescope from the Cassiopeia A [3] and (possibly) from the Vela supernova remnants [4] not only confirmed these ideas but also demonstrated that the ^{44}Ti gamma afterglow can be used to locate individual supernova remnants. It is expected that in the near future much scientific activity will be centered around ^{44}Ti . With the recent precise measurements of the ^{44}Ti half-life ($59.0 \pm 0.6 \text{ yr}$ [5], $60.3 \pm 1.3 \text{ yr}$ [6], $62 \pm 2 \text{ yr}$ [7], and $60.7 \pm 1.2 \text{ yr}$ [8]) and with the launch of the next-generation space-based gamma-ray observatory INTEGRAL [9] (scheduled for 2001), new supernova remnants are likely to be discovered and the total mass of ^{44}Ti ejected in the supernova events will be determined.

The use of the ^{44}Ti afterglow of supernovae for distance or age determination depends critically on the amount of ^{44}Ti produced in the explosion which is governed by a subtle interplay between the nuclear reactions that produce it and those that destroy it. This subject was studied in detail for type II supernovae by The *et al.* [10]. From these calculations, it was concluded that the amount of ^{44}Ti produced in a supernova depends strongly on the cross section of the $^{44}\text{Ti}(\alpha, p)^{47}\text{V}$ reaction.

Since the $^{44}\text{Ti}(\alpha, p)^{47}\text{V}$ reaction destroys ^{44}Ti , an increase in its rate will decrease the final amount of ^{44}Ti and vice versa. Because of the relatively high value of the Coulomb barrier for the $^4\text{He} + ^{44}\text{Ti}$ system, the influence of this reaction is felt at temperatures of $(2.2\text{--}4.2) \times 10^9 \text{ K}$. This temperature range corresponds to center-of-mass energies (Gamow peak values) of 4–6.1 MeV, or excitation energies of 11.7–13.8 MeV in the compound nucleus ^{48}Cr . Because the proton and neutron separation energies of ^{48}Cr are 5.17 and 16.33 MeV, respectively,

most of the fusion events will lead to ^{47}V , while only a few will result in α capture leading to ^{48}Cr . The cross sections for the $^{44}\text{Ti}(\alpha, p)$ reaction in this energy range are predicted to be 0.05–300 mb [11]. In order to put the nuclear astrophysics part of ^{44}Ti production in supernovae on a more solid ground we have performed the first measurement of the $^{44}\text{Ti}(\alpha, p)^{47}\text{V}$ reaction.

The long half-life of ^{44}Ti allows two approaches to a measurement of the $^{44}\text{Ti}(\alpha, p)^{47}\text{V}$ cross sections: a ^4He beam bombarding a ^{44}Ti target or a ^{44}Ti beam bombarding a ^4He target. Because of the higher energies of the reaction products in experiments with a ^{44}Ti beam, which strongly facilitates the particle identification, it was decided to develop a radioactive ^{44}Ti beam and to investigate the reaction in inverse kinematics, i.e., bombarding a ^4He target with a ^{44}Ti beam.

The ^{44}Ti material was produced via the $^{45}\text{Sc}(p, 2n)$ reaction [12,13], using a 50 MeV, 20 μA proton beam from the linac injector of Argonne's Intense Pulsed Neutron Source facility. The target, a 25 mm diam, 5 mm thick disk of Sc, was mounted inside a water-cooled Cu holder, whose front face was made of graphite, acting both as a collimator and an energy degrader. The irradiation lasted $\sim 70 \text{ h}$. Two weeks later, the Sc disk was removed from the holder and placed in front of a Ge detector. The dominant source of gamma radiation was found to result from the decay of ^{44}Sc . Nuclei of ^{46}Sc ($T_{1/2} = 83.8 \text{ d}$) were also produced by neutron capture. A ^{44}Ti activity of $\sim 180 \mu\text{Ci}$ was obtained from the γ spectrum, which represents $\sim 1.8 \times 10^{16}$ atoms or $\sim 1.3 \mu\text{g}$ of ^{44}Ti . About four weeks later, the ^{44}Ti activity was chemically separated from the Sc material. The method used for the chemical separation is similar to the ones used in Refs. [14,15]. The Sc disk was dissolved in a HNO_3/HCl solution and the Sc then precipitated out by the addition of HF. The solution containing the Ti activity was then dried and heated. A part of the resulting material, left as a $^{44}\text{TiO}_2$ compound,

was mixed with 50 mg of $^{nat}\text{TiO}_2$ and placed inside a copper insert for a negative-ion Cs-sputter source. The ^{44}Ti activity from the pellet was measured to be $\sim 38 \mu\text{Ci}$.

From the ion source a beam of $^{44}\text{TiO}^-$ was extracted and injected into the tandem accelerator at ATLAS. After stripping in the terminal of the tandem, a $^{44}\text{Ti}^{8+}$ beam was accelerated in the linac part of ATLAS to an energy of 133.5 MeV. Two guide beams were used to optimize the beam tuning of the ATLAS accelerator for the weak $^{44}\text{Ti}^{8+}$ beam: The optics of the ion source and the tandem injector were tuned with $^{48}\text{TiO}^-$, while the superconducting linac was tuned with $^{66}\text{Zn}^{12+}$.

Argonne's fragment mass analyzer (FMA) [16], a recoil mass separator dispersing the reaction products in its focal plane according to their m/q ratios, was used to separate the ^{47}V reaction products emitted at small scattering angles (typically $\leq 2^\circ$) from the primary mass 44 beam particles. To further separate the ^{47}V particles from the scattered beam an ionization chamber (IC) and a Si detector were placed behind the parallel grid avalanche counter (PGAC) at the focal plane of the FMA. The PGAC provided position and timing signals, while the IC-Si detectors gave energy and Z information.

To avoid a retuning of the linac at each energy change, which, for low intensity beams, can be quite time-consuming, Ti degrader foils ranging in thickness from 0.6 to 2 mg/cm^2 were used. The energy measurements of the beam were done by time of flight using the isochronous property of the FMA [16].

A ^4He gas target, a movable Si detector, a set of degrader foils, and a Au/C charge-reset foil after the target were mounted in the scattering chamber in front of the FMA. The ^4He gas target consisted of a 2.2 mm long cell with two 1.3 mg/cm^2 titanium metal windows, filled with 600 mbar of ^4He and cooled to LN_2 temperature. The areal density was 80 $\mu\text{g}/\text{cm}^2$. The main purpose of the Si detector in the scattering chamber was to monitor elastic scattering from the target for beam current normalization.

Before the ^{44}Ti experiment the experimental arrangement was tested with stable ^{40}Ca and ^{46}Ti beams. For ^{40}Ca as well as for ^{44}Ti , the (α, p) reaction dominates in the energy range of interest. With the charge state distributions from Ref. [17] and a transport efficiency through the FMA which was calculated taking the kinematics and small angle scattering into account, the measured excitation function for the $^{40}\text{Ca}(\alpha, p)^{43}\text{Sc}$ reaction was found to be in very good agreement with the results of Ref. [18].

Experiments with radioactive beams often have the added complication that these low-intensity beams have contaminations from neighboring isobars [19]. For ^{44}Ti the stable isobar is ^{44}Ca with a mass difference $\Delta M/M \sim 1.1 \times 10^{-4}$ which is too small to allow a separation by the beam transport system. In order to measure the composition of the mass 44 beam, a 2 mg/cm^2 Ti foil was used to degrade its energy and the FMA was set to separate the beam particles in m/q . Ti and Ca ions

experience a different energy loss in this foil and can thus be easily identified in the focal plane of the FMA. Figure 1 shows a Si energy vs IC energy plot where the different components of the beam are indicated. From these measurements it was concluded that 38% of the beam consisted of ^{44}Ti , 54% of ^{44}Ca , while ^{33}S and ^{11}B accounted for the remaining 8%. The ^{33}S and ^{11}B ions are injected as mass 60 molecules from the ion source and ions with the same charge-to-mass ratio are accelerated to the same velocity in the linear accelerator. Intensities of $\sim 5 \times 10^5$ $^{44}\text{Ti}/\text{s}$ on target were observed.

Plots of the time of flight through the FMA versus the energy measured in the Si detector behind the focal plane can be seen in Fig. 2 for an incident ^{44}Ti energy of 122.1 MeV. The left panel corresponds to an empty gas cell, the right one to a gas cell filled with 600 mbar of He. With the empty cell only mass 44 particles are observed, produced by scattering beam particles in the gas cell's windows or on various components in the FMA. The plot for the full gas cell shows the mass 47 reaction products, well separated from the scattered mass 44 particles. To measure the contributions from the reaction products from the ^{44}Ca component of the beam [mainly ^{47}Ti and ^{47}Sc produced via the $^4\text{He}(^{44}\text{Ca}, n)$ and $^4\text{He}(^{44}\text{Ca}, p)$ reactions] a pure beam of ^{44}Ca was used in the last stages of the experiment, repeating the measurements under identical experimental conditions. Elastically scattered particles were used to normalize the different runs to each other. The contribution of ^{47}V produced via the $^{44}\text{Ti}(\alpha, p)$ reaction to the total number of mass 47 reaction products depended on the incident energy and the charge state chosen for transmission through the FMA. The charge states for ^{47}V were 13^+ at the two highest energies and 12^+ and 11^+ at the two lower ones. The amount of ^{47}V in the mass

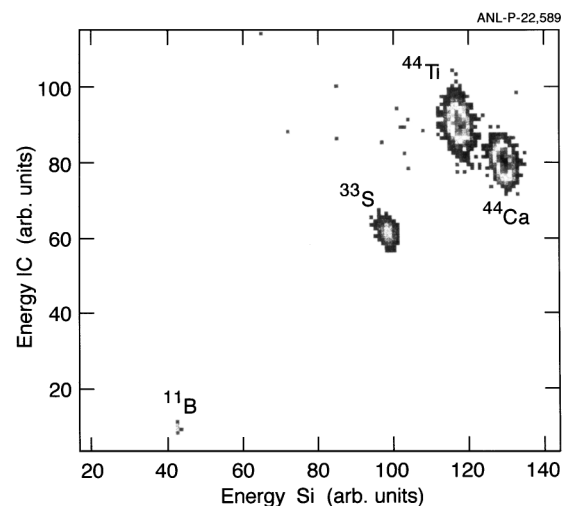


FIG. 1. Energy loss (measured in the ionization chamber) vs residual energy (measured in the Si detector) for particles detected in the focal plane of the fragment mass analyzer. The different components of the beam are indicated.

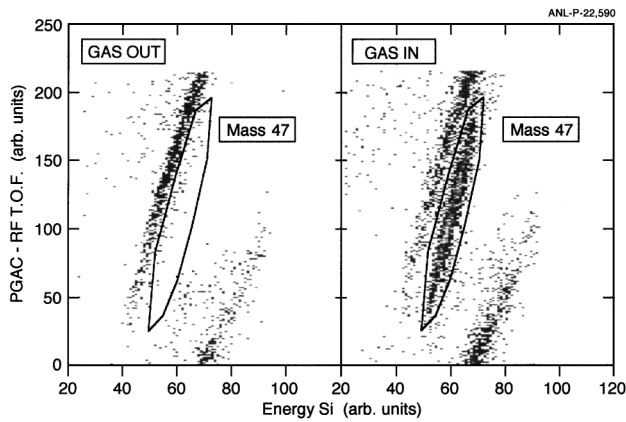


FIG. 2. Time of flight (measured with the parallel-grid-avalanche counter relative to the rf timing from the accelerator) vs energy (measured in the Si detector). The left panel corresponds to an empty gas cell, the one at the right to a full gas cell. The reaction products with mass 47 are indicated by the solid contour line.

47 gate was found to be 51%, 23%, 30%, and 48% for the c.m. energies of 9.0, 8.0, 6.8, and 5.7, respectively. To correct for the charge-state distribution of ^{47}V detected in the focal plane, the distributions were measured in a separate experiment using stable ^{51}V beams in the energy range $E_{\text{lab}} = 25\text{--}110$ MeV and adjusted to the same velocities. The resulting cross sections for the $^{44}\text{Ti}(\alpha, p)^{47}\text{V}$ reaction can be seen in Fig. 3. The error bars include statistical uncertainties as well as uncertainties from the ^{44}Ca beam contaminant, the charge state distributions, and transport efficiencies.

The solid line is the result (with standard parameters) from the statistical model code SMOKER [11] which is used

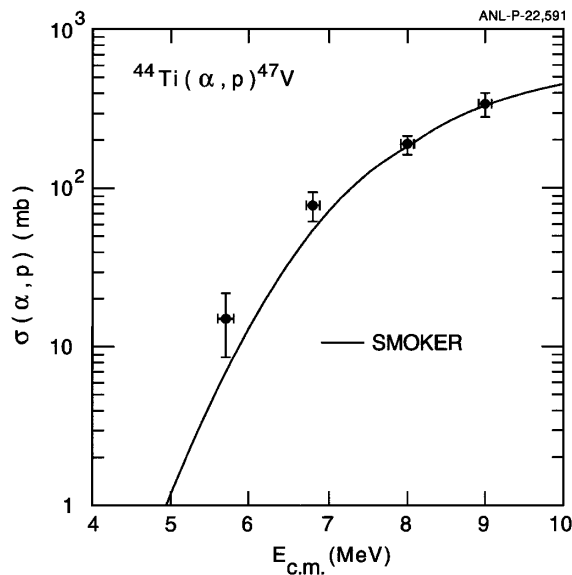


FIG. 3. Measured excitation function for the $^{44}\text{Ti}(\alpha, p)^{47}\text{V}$ reaction. The solid line corresponds to a calculation done with the code SMOKER (see text for details).

in many astrophysical network calculations to estimate astrophysical reaction rates that cannot be studied in the laboratory. At the two higher energies the agreement between our experiment and the theoretical prediction is excellent. However, the falloff in the cross section due to the penetration of the Coulomb barrier appears to be shifted towards lower energies resulting in cross sections that are larger by about a factor of 2 compared to the SMOKER predictions, thus implying a larger barrier radius or diffuseness parameter. It is interesting to note that a similar behavior is found for the neighboring $^{48}\text{Ti}(\alpha, n)^{51}\text{Cr}$ reaction [20] where a comparison with SMOKER shows good agreement for energies above 8 MeV, but a similar deviation at lower energies. Calculations with the newer code NONSMOKER [21] gave identical results.

In order to extract the astrophysical reaction rates, it is necessary to extrapolate the cross sections towards higher and lower energies. In this work, the cross sections were obtained by interpolating between the measured data points in the energy range $E_{\text{c.m.}} = 5.7\text{--}9.0$ MeV. For energies lower than 5.7 MeV or higher than 9.0 MeV, the cross sections were obtained by using the shape of the SMOKER calculation renormalized to match the lowest and highest measured data points. The results are shown by the solid line in Fig. 4. The uncertainties in the reaction rates range from 30% at the highest temperatures to 43% at $T_9 = 2.5$. The reaction rates from the SMOKER calculations as well as those by Woosley *et al.* [22] are given by the dashed and dot-dashed curves, respectively. These two sets of theoretical calculations give basically the same result for the $^{44}\text{Ti}(\alpha, p)^{47}\text{V}$ reaction rates, which is lower than the experimentally determined rate by about a factor of 2. The

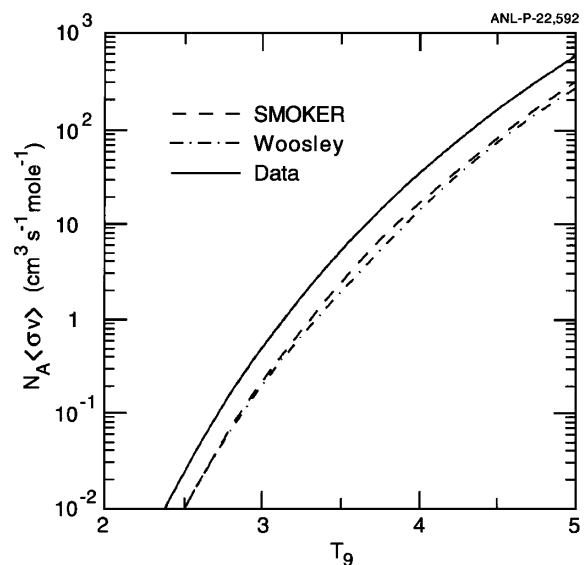


FIG. 4. Astrophysical reaction rates for the $^{44}\text{Ti}(\alpha, p)^{47}\text{V}$ reaction. The solid line was obtained from the experimental information as described in the text. The dashed line corresponds to a SMOKER calculation and the dot-dashed line to a calculation by Woosley *et al.* [22].

rate can be parametrized as a function of T_9 by the equation (see, e.g., Ref. [10,11])

$$N_A \langle \sigma v \rangle = \exp[A + B/T_9 + C/T_9^{1/3} + D \\ \times T_9^{1/3} + E \times T_9 + F \times T_9^{5/3} + G \\ \times \ln(T_9)], \quad (1)$$

with the parameters $A = -847.89$, $B = -167.79$, $C = 2142.3$, $D = -1179.5$, $E = 27.782$, $F = -0.70445$, and $G = 946.48$.

The higher astrophysical reaction rate results in a reduction of the amount of ^{44}Ti produced in supernovae explosions. Using the calculations of Ref. [10], one obtains with the higher reaction rate shown in Fig. 4 a 25% decrease in the ^{44}Ti yield of a type II supernova. For a measurement of the ^{44}Ti gamma-ray flux from a supernova, this decrease in yield translates into a 15% larger distance or a 25 yr earlier occurrence. It should be noted that changes in other reaction rates which have not been measured so far [e.g., the $^{45}\text{V}(p, \gamma)$ reaction] could effect the ^{44}Ti yield as well. A more detailed study of the influence of the higher rate of ^{44}Ti destruction on searches for ^{44}Ti decay γ rays from supernovae remains to be done.

In addition to its effects on the energetics of the light curve of supernova 1987A, and for searches for ^{44}Ti decay γ rays from galactic supernova remnants, these new experimental results also hold important implications for galactic nucleosynthesis. Observational determinations of the abundances of (elemental) titanium in the oldest (most metal deficient) stars in our galaxy [23] reveal that, like the "alpha elements" oxygen, neon, magnesium, silicon, sulfur, argon, and calcium, titanium is overabundant relative to iron by a factor of $\approx 2-3$. This is understood to reflect the nucleosynthesis products of supernovae of type II, which are associated with the evolution of massive stars of short lifetimes [24]. The most abundant naturally occurring isotope of titanium, ^{48}Ti , is formed in such supernovae as ^{48}Cr , under conditions which are equivalent to those giving rise to the formation of ^{56}Ni [25,26]. Preliminary calculations of supernova nucleosynthesis utilizing our higher rate for $^{44}\text{Ti}(\alpha, p)^{47}\text{V}$ indicate that a higher level of ^{48}Cr production may accompany oxygen burning and/or incomplete silicon burning.

We thank Thomas Rauscher for providing us with the SMOKER and NONSMOKER cross section calculations. This work was supported by the U.S. Department of Energy,

Nuclear Physics Division, under Contract No. W-31-109-ENG-38.

-
- [1] David Arnett, *Supernovae and Nucleosynthesis* (Princeton University Press, Princeton, NJ, 1996).
 - [2] M.D. Leising, Nucl. Phys. **A621**, 71c (1997); C. Dupraz *et al.*, Astron. Astrophys. **324**, 683 (1997).
 - [3] A.F. Iyudin *et al.*, Astron. Astrophys. **284**, L1 (1994).
 - [4] A.F. Iyudin *et al.*, Nature (London) **396**, 142 (1998).
 - [5] I. Ahmad *et al.*, Phys. Rev. Lett. **80**, 2550 (1998).
 - [6] J. Görres *et al.*, Phys. Rev. Lett. **80**, 2554 (1998).
 - [7] E.B. Norman *et al.*, Phys. Rev. C **57**, 2010 (1998).
 - [8] F.E. Wiefeldt *et al.*, Phys. Rev. C **59**, 528 (1999).
 - [9] International Gamma-Ray Astrophysics Laboratory, <http://sci.esa.int/integral/>.
 - [10] L.-S. The *et al.*, Astrophys. J. **504**, 500 (1998).
 - [11] F.-K. Thielemann, M. Arnould, and J.W. Truran, in *Advances in Nuclear Astrophysics*, edited by E. Vangioni-Flam *et al.* (Editions Frontieres, Gif-sur-Yvette, 1987), p. 525.
 - [12] T. McGee *et al.*, Nucl. Phys. **A150**, 11 (1970).
 - [13] R. Ejnisman *et al.*, Phys. Rev. C **54**, 2047 (1996).
 - [14] D. Frekers *et al.*, Phys. Rev. C **28**, 1756 (1983).
 - [15] R. Lange *et al.*, Nucl. Instrum. Methods Phys. Res., Sect. A **423**, 247 (1999).
 - [16] C.N. Davids *et al.*, Nucl. Instrum. Methods Phys. Res., Sect. B **70**, 358 (1992).
 - [17] K. Shima, T. Mikumo, and H. Tawara, At. Data Nucl. Data Tables **34**, 357 (1986).
 - [18] A.J. Howard *et al.*, Astrophys. J. **188**, 131 (1974).
 - [19] K.E. Rehm *et al.*, Phys. Rev. Lett. **80**, 676 (1998).
 - [20] H. Vonach, R.C. Haight, and G. Winkler, Phys. Rev. C **28**, 2278 (1983).
 - [21] T. Rauscher, F.-K. Thielemann, and K.-L. Kratz, Phys. Rev. C **56**, 1613 (1997); T. Rauscher and F.-K. Thielemann, At. Data Nucl. Data Tables (to be published).
 - [22] S.E. Woosley *et al.*, At. Data Nucl. Data Tables **22**, 371 (1978).
 - [23] J.C. Wheeler, C. Sneden, and J.W. Truran, Annu. Rev. Astron. Astrophys. **27**, 279 (1989).
 - [24] S.E. Woosley and T.A. Weaver, Astrophys. J. Suppl. **101**, 181 (1995).
 - [25] J.W. Truran, W.D. Arnett, and A.G.W. Cameron, Can. J. Phys. **45**, 2315 (1967).
 - [26] S.E. Woosley and T.A. Weaver, in *Supernovae*, Proceedings of the Les Houches Summer School, Session LIV, edited by J. Audouze *et al.* (Elsevier, New York, 1999), p. 63.